Entanglement between electronic and vibrational degrees of freedom in a laser-driven molecular system

Mihaela Vatasescu*
Institute of Space Sciences - INFLPR, MG-23, 77125 Bucharest-Magurele, Romania
(Received 20 August 2013; published 23 December 2013)

We investigate the entanglement between electronic and vibrational degrees of freedom produced by a vibronic coupling in a molecular system described in the Born-Oppenheimer approximation. Entanglement in a pure state of the Hilbert space $\mathcal{H} = \mathcal{H}_{\rm el} \bigotimes \mathcal{H}_{\rm vib}$ is quantified using the von Neumann entropy of the reduced density matrix and the reduced linear entropy. Expressions for these entanglement measures are derived for the $2 \times N_v$ and $3 \times N_v$ cases of the bipartite entanglement, where 2 and 3 are the dimensions of the electronic Hilbert space $\mathcal{H}_{\rm el}$, and N_v is the dimension of $\mathcal{H}_{\rm vib}$. We study the entanglement dynamics for two electronic states coupled by a laser pulse (a $2 \times N_v$ case), taking as an example a coupling between the $a^3\Sigma_u{}^+(6s,6s)$ and $1_g(6s,6p_{3/2})$ states of the Cs_2 molecule. The reduced linear entropy expression obtained for the $3 \times N_v$ case is used to follow the entanglement evolution in a scheme proposed for the control of the vibronic dynamics in a Cs_2 cold molecule, implying the $a^3\Sigma_u{}^+(6s,6s)$, $0_g{}^-(6s,6p_{3/2})$, and $0_g{}^-(6s,5d)$ electronic states, which are coupled by a nonadiabatic radial coupling and a sequence of chirped laser pulses.

DOI: 10.1103/PhysRevA.88.063415 PACS number(s): 33.80.Be, 03.67.Bg, 03.65.Ud, 33.15.Vb

I. INTRODUCTION

Quantum entanglement, central to the foundations of quantum theory [1], is today a reference concept shaping the understanding of various quantum phenomena in physics, chemistry, and quantum biology. With the emergence of quantum information theory entanglement was also recognized as a fundamental resource for quantum computation and quantum communication [2].

In the last 20 years atomic and molecular physics had a particularly fortunate encounter with quantum information theory, sustained by the continuous development of experimental techniques able to produce extremely controllable ultracold atomic and molecular systems. Entanglement has been explored in a variety of experiments employing highly controlled atomic systems like cold trapped ions [3], Rydberg atoms crossing a "photon box" [4], or neutral atoms in optical lattices [5]. The controlled creation of entanglement between pairs of atoms trapped in an optical lattice was used for precision measurements of atomic scattering properties [6], atomic spectroscopy using quantum logic was implemented with trapped atomic ions [7], and quantum metrology was performed using "designer atoms" [8]. A similar trend becomes increasingly possible in molecular physics, due to the progress in the formation of ultracold molecules. Proposals for molecular entanglement creation are considering ultracold polar molecules [9] as interesting systems for quantum information manipulation and promising platforms for quantum computation.

In addition to these developments there is also an increased interest in using quantum entanglement and quantum information concepts to describe the structure of atoms and molecules and related phenomena. A recent review focusing on "essential entanglement for atomic and molecular physics" [10] shows the specificity of this research program which considers physical objects far from the idealized systems familiar from the quantum information science and for which the identification of subsystems which can carry entanglement is nontrivial. Within this program various theoretical investigations have been advanced, including studies of entanglement in two-electron atomic systems [11] and investigations of the entanglement between the internal electronic and the external translational degrees of freedom of trapped atoms [12]. Studies of entanglement in molecular systems have considered the entanglement associated with the dissociation of diatomic molecules [13], entanglement in Rydberg molecules [14], and dynamical entanglement of vibrations in triatomic molecules [15].

Proposals for quantum computing using molecular internal degrees of freedom (electronic, vibrational, and rotational) have opened the door to stimulative research in molecular systems driven by shaped light pulses, in which optimal quantum control theory is used to find the driving fields which play the role of quantum logic gates [16]. These developments have stimulated the interest in the characterization of entanglement in laser-driven molecular systems.

The present work investigates the entanglement between electronic and nuclear degrees of freedom in a molecule. Few studies have treated this subject and these works consider Hilbert spaces with low dimensionality. Special attention is attached to double-welled chemical systems, as embodying electronic-vibrational entanglement through the role played by the wave-function delocalization [17,18], and to entanglement in relation with quantum chaos induced by nonadiabatic interaction due to the breakdown of the Born-Oppenheimer approximation [19].

Here we consider a molecular system (diatomic molecule) described in the Born-Oppenheimer (BO) approximation which separates the electronic and nuclear motion, leading to the factorization of the molecular wave function into an electronic and a rotational-vibrational part. The rotational degree of freedom is neglected, and, therefore, the system can be described by a Hilbert space which is a tensor product $\mathcal{H} = \mathcal{H}_{\rm el} \bigotimes \mathcal{H}_{\rm vib}$ of electronic and vibrational Hilbert spaces of finite dimensions. We will analyze the entanglement between

*mihaela_vatasescu@yahoo.com

electronic and vibrational degrees of freedom produced by a coupling between electronic states: this coupling could be produced by an external source, such as laser pulses acting on the molecular system, or it could be a nonadiabatic interaction neglected in the Born-Oppenheimer approximation. We consider pure states of the bipartite system (el $\bigotimes$ vib), and quantify the entanglement using the von Neumann entropy of the reduced density matrix and the linear entropy related to the purity of the reduced density matrix. We derive formulas for these measures of entanglement, which can be employed to follow the entanglement evolution in relation to the intramolecular dynamics.

We show results for the entanglement dynamics in two cases of temporal evolution in a laser-driven molecule. A first example treats the case of a laser coupling between the $a^3\Sigma_u{}^+(6s,6s)$ and $1_g(6s,6p_{3/2})$ electronic states of the Cs_2 molecule (a $2 \times N_v$ case). The second example follows the entanglement evolution quantified by the linear entropy (a $3 \times N_v$ case) in a theoretical control scheme proposed to create Cs_2 vibrationally cold molecules using a multichannel tunneling observed in the cesium photoassociation spectrum. The scheme employs the electronic states $a^3\Sigma_u{}^+(6s,6s)$, $0_g{}^-(6s,6p_{3/2})$, and $0_g{}^-(6s,5d)$ of the Cs_2 molecule, which are coupled by a nonadiabatic radial coupling and a sequence of chirped laser pulses. In both cases the entanglement dynamics is analyzed in relation to the characteristic times specific to the vibronic couplings and intramolecular dynamics.

The structure of the paper is as follows. Section II briefly reviews the theoretical framework of the BO approximation. In Sec. III the $2 \times N_v$ case of the bipartite entanglement is studied and expressions for the reduced von Neumann entropy and reduced linear entropy are derived. The example of two electronic states coupled by a laser pulse is contained in Sec. III B. Section IV treats the $3 \times N_v$ case, deducing the corresponding formula for the reduced linear entropy. Section V follows the entanglement evolution quantified by the linear entropy in the theoretical control scheme proposed to create Cs_2 vibrationally cold molecules using a sequence of chirped laser pulses. Section VI contains our final remarks.

II. MOLECULAR MODEL: BORN-OPPENHEIMER APPROXIMATION AND VIBRONIC COUPLINGS BETWEEN ELECTRONIC STATES

We briefly review some basic notions used in the description of a diatomic molecule in the BO approximation [20]. The mass difference between nuclei and electrons justifies the so-called clamped nuclei electronic Schrödinger equation, written for the electronic Hamiltonian $H^{\rm el}$ (i.e., the total molecular Hamiltonian without the nuclear kinetic-energy part):

$$H^{\rm el}\phi_n^{\rm el}(\vec{r}_i;R) = U_n(R)\phi_n^{\rm el}(\vec{r}_i;R), \tag{1}$$

where R is the internuclear distance and $\{\vec{r}_i\}$ the electronic coordinates expressed in the molecule-fixed coordinate system. This equation produces the adiabatic potential-energy surfaces $U_n(R)$ as eigenvalues of the electronic Hamiltonian and the electronic wave functions $\phi_n^{\rm el}(\vec{r}_i;R)$, depending parametrically on R, as orthonormal eigenstates of $H^{\rm el}$.

The molecular rovibronic wave function $\Psi_{\rm mol}(\vec{R},\vec{r}_i;t)$ can be expanded in the basis set of the electronic eigenfunctions $\{\phi_n^{\rm el}(\vec{r}_i;R)\}$:

$$\Psi_{\rm mol}(\vec{R},\vec{r}_i;t) = \sum_n \psi_n(\vec{R};t)\phi_n^{\rm el}(\vec{r}_i;R). \tag{2}$$

In Eq. (2) we have introduced the time-dependent picture emphasizing that the temporal dependence is contained in the nuclear wave functions $\psi_n(\vec{R};t)$. In a stationary picture, the coefficients $\psi_n(\vec{R})$ depending on the nuclear geometry are the rotational-vibrational wave functions. If the expansion (2) is inserted in the Schrödinger equation of the full molecular Hamiltonian, one obtains a system of coupled differential equations describing the motion of the nuclei in an electronic state, coupled with the nuclear motion in all other electronic states. In the BO approximation this coupling with other electronic states is neglected, providing a good description if the electronic wave functions depend only weakly on R. Then, the sum in Eq. (2) can be reduced to a single term:

$$\Psi_{\rm mol}(\vec{R},\vec{r}_i;t) \approx \psi_n(\vec{R};t)\phi_n^{\rm el}(\vec{r}_i;R). \tag{3}$$

This factorization of the total wave function into an electronic and a rotational-vibrational part is essential to the BO approximation. The consequence is that the nuclear motion in an electronic state is uniquely determined by the corresponding electronic potential, which allows one to write a rotational-vibrational Schrödinger equation for each electronic state. As the radial and angular variables of the nuclear motion can be also separated, the Schrödinger equation which defines the rovibrational eigenfunctions $\chi^n_{v,J}(R)$ corresponding to an electronic potential $U_n(R)$ can take the form

$$\left(-\frac{\hbar^2}{2\mu}\frac{\partial^2}{\partial R^2} + U_n(R) + \frac{\hbar^2 J(J+1)}{2\mu R^2}\right)\chi^n_{v,J}(R) = E^n_{v,J}\chi^n_{v,J}(R), \tag{4}$$

where μ is the nuclear reduced mass, J quantifies the rotational angular momentum, and $E^n_{v,J}$ are the energies of the rovibrational levels corresponding to the electronic state n.

Due to the fact that here the rotational degree of freedom is neglected the molecular system is described by the Hilbert space $\mathcal{H} = \mathcal{H}_{\rm el} \bigotimes \mathcal{H}_{\rm vib}$. The molecular wave function corresponding to an electronic state n, BO factored into electronic and vibrational wave functions, is

$$\Psi^n_{\rm mol}(R,\vec{r}_i,t) = \frac{1}{R}\chi_n(R,t)\phi_n^{\rm el}(R;\vec{r}_i) = \frac{1}{R}\left(\sum_v c_v^n(t)\chi_v^n(R)\right)\phi_n^{\rm el}(R;\vec{r}_i). \tag{5}$$

In Eq. (5) the vibrational wave packet $\chi_n(R,t)$ is developed in the orthonormal basis set of the vibrational eigenstates $\{\chi_v^n(R)\}$ corresponding to the electronic potential $U_n(R)$. $\{\chi_v^n(R)\}$ are solutions of Eq. (4) for $J = 0$ or for fixed J.

The BO states are generally those on which the molecular description is built[1] by including various coupling mechanisms between the electronic states, such as non-BO coupling

[1]"In order to go beyond the BO approximation, it is necessary to use a BO representation," as it is expressed in Ref. [20].

terms subsequently introduced in the description, or vibronic couplings caused by external fields. In the following we consider a molecular system which can be described by a pure state belonging to the bipartite Hilbert space $\mathcal{H}_{\rm el} \bigotimes \mathcal{H}_{\rm vib}$ of finite dimension. Our aim is to derive formulas for the entanglement between electronic and vibrational degrees of freedom produced by vibronic couplings of the electronic states. In the next sections we will explore the cases of bipartite entanglement in pure states belonging to Hilbert spaces of $2 \times N_v$ and $3 \times N_v$ dimensions.

III. MEASURES OF ENTANGLEMENT BETWEEN ELECTRONIC AND VIBRATIONAL DEGREES OF FREEDOM IN A $2 \times N_v$ MOLECULAR SYSTEM

Considering two coupled electronic states (g,e), our aim is to derive an expression for the electronic-nuclear entanglement produced by the vibronic coupling. We are especially interested in describing cases of coupling due to a laser pulse, but the nature of the coupling does not need to be specified in the formal part of our treatment. The only restriction that we employ is that the coupling creates a pure state in the Hilbert space $\mathcal{H} = \mathcal{H}_{\rm el} \bigotimes \mathcal{H}_{\rm vib}$ of dimension $2 \times N_v$, whose wave function can be written as

$$\Psi_{\rm el,vib}(R,\vec{r}_i;t) = \phi_g^{\rm el}(\vec{r}_i;R)\psi_g(R,t) + \phi_e^{\rm el}(\vec{r}_i;R)\psi_e(R,t). \tag{6}$$

If $\{|\chi_{v_g}(R)\rangle\}_{v_g=\overline{1,N_g}}$ and $\{|\chi_{v_e}(R)\rangle\}_{v_e=\overline{1,N_e}}$ are the orthonormal vibrational bases with dimensions N_g and N_e ($N_g + N_e = N_v$), corresponding to the electronic surfaces g,e, respectively, Eq. (6) can be rewritten as

$$|\Psi_{\rm el,vib}(t)\rangle = |g\rangle \bigotimes \sum_{v_g=1}^{N_g} c_{v_g}(t)\left|\chi_{v_g}\right\rangle + |e\rangle \bigotimes \sum_{v_e=1}^{N_e} c_{v_e}(t)\left|\chi_{v_e}\right\rangle, \tag{7}$$

where $|g\rangle$, $|e\rangle$ designate the electronic states $\phi_{g,e}^{\rm el}(\vec{r}_i;R)$, and the nuclear wave packets $\psi_{g,e}(R,t)$ were developed in their corresponding vibrational bases. The complex coefficients $\{c_{v_g}(t)\},\{c_{v_e}(t)\}$ give the population probabilities $\{|c_{v_g}(t)|^2\},\{|c_{v_e}(t)|^2\}$ of the vibrational levels $\{v_g\}$ and $\{v_e\}$. For a closed system comprised of only these two electronic surfaces, the normalization condition $\langle\Psi_{\rm el,vib}(t)|\Psi_{\rm el,vib}(t)\rangle = 1$ is expressed by the relation

$$\sum_{v_g=1}^{N_g}\left|c_{v_g}(t)\right|^2 + \sum_{v_e=1}^{N_e}\left|c_{v_e}(t)\right|^2 = 1, \tag{8}$$

and the density operator

$$\hat{\rho}_{\rm el,vib}(t) = |\Psi_{\rm el,vib}(t)\rangle\langle\Psi_{\rm el,vib}(t)| \tag{9}$$

corresponds to a pure state of the bipartite system: $\hat{\rho}^2_{\rm el,vib} = \hat{\rho}_{\rm el,vib}$.

Pure bipartite states have clear separability criteria like the Schmidt decomposition [1,21], and "good" measures of the amount of entanglement, the first one being the von Neumann entropy of the reduced density matrix [22,23]. Even if the von Neumann entropy of the subsystem is the "entropy of entanglement" [24] for pure states, and it could be considered as "the unique measure for pure states" [1], it was also argued that "only one measure is not sufficient to completely quantify entanglement of pure states for bipartite systems," and "several independent measures should be employed simultaneously" [25]. In the present work we shall refer to two measures quantifying the entanglement: the von Neumann entropy and the linear entropy of the reduced density matrix.

To estimate the entanglement of $|\Psi_{\rm el,vib}(t)\rangle$, we have to analyze the reduced density operator of one of the two subsystems: $\hat{\rho}_{\rm el} = {\rm Tr}_{\rm vib}(\hat{\rho}_{\rm el,vib})$ or $\hat{\rho}_{\rm vib} = {\rm Tr}_{\rm el}(\hat{\rho}_{\rm el,vib})$. The spectrum of the reduced density matrix (for example $\hat{\rho}_{\rm el}$) gives the Schmidt coefficients which allow us to distinguish separable from entangled states and can be used to obtain the von Neumann entropy $S_{vN}(\hat{\rho}_{\rm el})$. On the other hand, the purity of the reduced density, ${\rm Tr}\hat{\rho}^2_{\rm el}$, shows the degree of mixing of the subsystems and is also an indicator for the degree of entanglement in system: if ${\rm Tr}\hat{\rho}^2_{\rm el} \neq 1$ the state described by Eq. (7) is entangled [26].

In order to obtain a reduced density matrix one needs to designate an orthonormal basis set for each subsystem Hilbert space, $\mathcal{H}_{\rm el}$ and $\mathcal{H}_{\rm vib}$. $\{|g\rangle,|e\rangle\}$ constitutes such a basis set for $\mathcal{H}_{\rm el}$. In $\mathcal{H}_{\rm vib}$ we have the two vibrational bases $\{|\chi_{v_g}(R)\rangle\}_{v_g=\overline{1,N_g}}$ and $\{|\chi_{v_e}(R)\rangle\}_{v_e=\overline{1,N_e}}$, but generally $\langle\chi_{v_g}(R)|\chi_{v_e}(R)\rangle \neq 0$, so we need to construct a complete orthonormal vibronic basis $\{|j\rangle\}_{j=1,N_v}$ of $\mathcal{H}_{\rm vib}$, which will have the dimension $N_v = N_g + N_e$ and will satisfy the orthonormality ($\langle j|j'\rangle = \delta_{jj'}$) and completeness ($\sum_{j=1}^{N_v}|j\rangle\langle j| = \hat{I}_v$) conditions. Then, designating by $\{|1\rangle,|2\rangle\}$ a suited orthonormal basis in the electronic Hilbert space $\mathcal{H}_{\rm el}$, $|\Psi_{\rm el,vib}(t)\rangle$ can be also expressed as

$$|\Psi_{\rm el,vib}(t)\rangle = |1\rangle \bigotimes \sum_{j=1}^{N_v} C_{1j}(t)|j\rangle + |2\rangle \bigotimes \sum_{j=1}^{N_v} C_{2j}(t)|j\rangle. \tag{10}$$

The complex coefficients C_{1j},C_{2j} obey a normalization condition similar to Eq. (8):

$$\sum_{j=1}^{N_v}[|C_{1j}(t)|^2 + |C_{2j}(t)|^2] = 1. \tag{11}$$

The reduced density operator $\hat{\rho}_{\rm el}$ can now be calculated using the vibronic basis $\{|j\rangle\}_{j=1,N_v}$:

$$\hat{\rho}_{\rm el}(t) = {\rm Tr}_{\rm vib}[|\Psi_{\rm el,vib}(t)\rangle\langle\Psi_{\rm el,vib}(t)|] = \sum_{j=1}^{N_v}\langle j|\Psi_{\rm el,vib}(t)\rangle\langle\Psi_{\rm el,vib}(t)|j\rangle, \tag{12}$$

and the reduced density matrix $(\hat{\rho}_{\rm el})$ can be expressed in the electronic basis $\{|1\rangle,|2\rangle\}$ as

$$(\hat{\rho}_{\rm el}) = \begin{pmatrix} \sum_j |C_{1j}|^2 & \sum_j C_{1j}C^*_{2j} \\ \sum_j C^*_{1j}C_{2j} & \sum_j |C_{2j}|^2 \end{pmatrix}, \tag{13}$$

where the summation is over $j = \overline{1,N_v}$, and ${\rm Tr}(\hat{\rho}_{\rm el}) = 1$.

To express the quantities implying the coefficients C_{1j}, C_{2j} as functions of entities related to the initial electronic states g, e, we choose the new electronic basis set as

$$|1\rangle = \frac{1}{\sqrt{2}}(|g\rangle + |e\rangle), \quad |2\rangle = \frac{1}{\sqrt{2}}(|g\rangle - |e\rangle). \tag{14}$$

Using Eqs. (7), (10), (14) together with the orthornormality and completeness relations, the quantities implying the coefficients C_{1j}, C_{2j} can be expressed as functions of $c_{v_g}(t)$, $c_{v_e}(t)$ and of the vibrational eigenstates $|\chi_{v_g}\rangle$, $|\chi_{v_e}\rangle$.

The eigenvalues of the matrix (13) are $\rho_{+,-}(t) = \frac{1}{2}\{1 \pm [P_g(t) - P_e(t)]\}$, with $P_g(t) = \sum_{v_g} |c_{v_g}(t)|^2$ and $P_e(t) = \sum_{v_e} |c_{v_e}(t)|^2$ being the vibrational populations of the g, e electronic states. As $P_g(t) + P_e(t) = 1$, the eigenvalues of the reduced density matrix ($\hat{\rho}_{\rm el}$) are simply the populations of the electronic states:

$$\rho_+(t) = P_g(t), \quad \rho_-(t) = P_e(t). \tag{15}$$

Knowing that the eigenvalues $\rho_{+,-}(t)$ are the squares of the coefficients defining the Schmidt decomposition of the pure bipartite state $|\Psi_{\rm el,vib}(t)\rangle$ [1,21], one reaches the easily understandable conclusion that separability appears if only one of the electronic states is populated [$P_g(t) = 1$ and $P_e(t) = 0$, or vice versa], and maximum entanglement is realized for $P_g(t) = P_e(t) = 1/2$.

To advance to the dynamical aspects of entanglement, one has to use measures such as the von Neumann entropy of the reduced density matrix or the linear entropy (calculated via the purity of the reduced density matrix). The von Neumann entropy of entanglement

$$S_{vN}(\hat{\rho}_{\rm el}) = -{\rm Tr}(\hat{\rho}_{\rm el} \log_2 \hat{\rho}_{\rm el}) \tag{16}$$

is the Shannon entropy of the squares of the Schmidt coefficients [24]: $S_{vN}(\hat{\rho}_{\rm el}) = -\rho_+ \log_2 \rho_+ - \rho_- \log_2 \rho_-$. Two alternative expressions can be written:

$$S_{vN}(\hat{\rho}_{\rm el}(t)) = -P_g(t) \log_2 P_g(t) - P_e(t) \log_2 P_e(t) \tag{17a}$$

$$= -\frac{1 + D(t)}{2} \log_2 \frac{1 + D(t)}{2} - \frac{1 - D(t)}{2} \log_2 \frac{1 - D(t)}{2}. \tag{17b}$$

The notation $D(t) = P_g(t) - P_e(t)$ was employed in deriving (17b), which is the form taken by the von Neumann entropy for the density operator of a qubit, $D(t)$ being the module of the Bloch vector [26].

As expected, the von Neumann entropy $S_{vN}(\hat{\rho}_{\rm el}(t))$ is 0 for a separable state (if one of the eigenvalues is 1, the other being 0), and attains the maximum value 1 for maximum entanglement [when $P_g(t) = P_e(t) = 1/2$]. It is important to notice that Eq. (17a) gives the possibility to investigate the entanglement dynamics in a molecular process.

Now we shall analyze the purity of the reduced density matrix, ${\rm Tr}[\hat{\rho}^2_{\rm el}(t)]$, which is related to the linear entropy of entanglement $L(t)$:

$$L(t) = 1 - {\rm Tr}\big[\hat{\rho}^2_{\rm el}(t)\big]. \tag{18}$$

Using Eq. (13) one obtains

$${\rm Tr}\big(\hat{\rho}^2_{\rm el}\big) = \left(\sum_{j=1}^{N_v} |C_{1j}|^2\right)^2 + \left(\sum_{j=1}^{N_v} |C_{2j}|^2\right)^2 + 2\left|\sum_{j=1}^{N_v} C_{1j} C^*_{2j}\right|^2. \tag{19}$$

These quantities can be written as functions of $c_{v_g}(t)$, $c_{v_e}(t)$, $|\chi_{v_g}\rangle$, $|\chi_{v_e}\rangle$, to reach the expression

$${\rm Tr}\big[\hat{\rho}^2_{\rm el}(t)\big] = \frac{1}{2} + \frac{1}{2}[P_g(t) - P_e(t)]^2 + 2\left|\sum_{v_g=1}^{N_g}\sum_{v_e=1}^{N_e} c^*_{v_g}(t) c_{v_e}(t) \langle \chi_{v_g}(R) \big| \chi_{v_e}(R)\rangle\right|^2. \tag{20}$$

Using the condition $P_g(t) + P_e(t) = 1$, and writing the vibrational wave packet in an electronic state as

$$|\psi(R,t)\rangle = \sum_v c_v(t) |\chi_v(R)\rangle, \tag{21}$$

Eq. (20) takes the simple form

$${\rm Tr}\big[\hat{\rho}^2_{\rm el}(t)\big] = P^2_g(t) + P^2_e(t) + 2|\langle \psi_g(R,t) | \psi_e(R,t)\rangle|^2. \tag{22}$$

Equations (20) and (22) show the purity ${\rm Tr}[\hat{\rho}^2_{\rm el}(t)]$ as an interesting sensor for the correlations between the electronic channels, emphasizing explicitly the role played by the vibronic coherences. The purity defined by Eq. (20) is bounded by $\frac{1}{2} \leqslant {\rm Tr}[\hat{\rho}^2_{\rm el}(t)] \leqslant 1$,[2] and the corresponding linear entropy by $0 \leqslant L(t) \leqslant \frac{1}{2}$. If ${\rm Tr}[\hat{\rho}^2_{\rm el}(t)] = 1$ [and $L(t) = 0$] the electronic subsystem is pure by itself, and then the pure bipartite state is nonentangled. It is, obviously, the result obtained with the relation (20) if only one of the electronic states is populated [all $c_{v_g}(t) = 0$ or all $c_{v_e}(t) = 0$].

These results show that an interaction between two electronic channels which leaves both channels populated will produce an entangled state, entanglement being present at all times if both channels remain populated.

In the following, we will use the expressions obtained for $S_{vN}(\hat{\rho}_{\rm el}(t))$, ${\rm Tr}[\hat{\rho}^2_{\rm el}(t)]$, and $L(t)$[3] to analyze the entanglement dynamics in specific cases of coupling of two electronic channels by a laser pulse.

[2]Generally, the purity ${\rm Tr}\hat{\rho}^2$ of a quantum state is bounded by $\frac{1}{d} \leqslant {\rm Tr}\hat{\rho}^2 \leqslant 1$, where d is the dimension of the Hilbert space attributed to the system [27].

[3]Comparing entanglement measures is obviously a subtle and complicated matter. We just make the observation that the von Neumann entropy $S_{vN}(\hat{\rho})$ and the purity ${\rm Tr}(\hat{\rho}^2)$ are both related to the quantum α Renyi entropies $S_\alpha(\hat{\rho}) = (1-\alpha)^{-1} \log_2 {\rm Tr}\hat{\rho}^\alpha$. In the limit $\alpha \to 1$, one obtains the entropy of entanglement: $S_1(\hat{\rho}) = S_{vN}(\hat{\rho})$. On the other hand, $S_2(\hat{\rho}) = -\log_2 {\rm Tr}(\hat{\rho}^2)$. Nevertheless, the Renyi entropies for $\alpha > 1$ do not have the same mathematical properties as those with $0 \leqslant \alpha \leqslant 1$, which fulfill the maximum of postulates required for an entanglement measure [1,25].

A. Entanglement dynamics produced by a constant vibronic coupling in a 2 × 2 system: One vibrational level in each electronic state

We consider first the model case of two electronic states g,e coupled by an electric field with amplitude $\mathcal{E}(t) = \mathcal{E}_0 \cos\omega_L t$. In the rotating wave approximation, the evolution of such a system is described by a time-dependent Schrödinger equation like Eq. (29), but with constant coupling W_L [28]. Considering a 2×2 system with one vibrational state associated with every electronic state, the "vibrational wave packets" associated with the electronic states are $|\psi_g(R,t)\rangle = c_{v_g}(t)|\chi_{v_g}(R)\rangle$ and $|\psi_e(R,t)\rangle = c_{v_e}(t)|\chi_{v_e}(R)\rangle$ [with $|c_{v_g}(t)|^2 + |c_{v_e}(t)|^2 = 1$]. In this case one can write an analytic expression for the population $|c_{v_e}(t)|^2$, showing the Rabi beats induced by the coupling between the two vibrational states with energies E_{v_e}, E_{v_g} [29]:

$$|c_{v_e}(t)|^2 = \frac{|W_L \mathcal{F}_{v_g v_e}|^2}{(\hbar\Omega_{v_e,v_g})^2} \sin^2(\Omega_{v_e,v_g} t), \tag{23}$$

$$\hbar\Omega_{v_e,v_g} = \sqrt{|W_L \mathcal{F}_{v_g v_e}|^2 + [(E_{v_e} - E_{v_g})/2]^2}. \tag{24}$$

In Eqs. (23) and (24) $|\mathcal{F}_{v_g v_e}|^2$ is the Franck-Condon factor, with $\mathcal{F}_{v_g v_e} = \langle\chi_{v_g}(R)|\chi_{v_e}(R)\rangle$ the overlap integral of the vibrational wave functions.

The eigenvalues of the reduced density matrix $\hat{\rho}_{\rm el}(t)$ are the populations of the two electronic states: $\rho_+(t) = P_g(t) = |c_{v_g}(t)|^2$, $\rho_-(t) = P_e(t) = |c_{v_e}(t)|^2$. Then, according to Eqs. (17) and (20), the von Neumann entropy and the purity are

$$S_{vN}(\hat{\rho}_{\rm el}(t)) = -|c_{v_g}(t)|^2 \log_2 |c_{v_g}(t)|^2 - |c_{v_e}(t)|^2 \log_2 |c_{v_e}(t)|^2, \tag{25}$$

$$\mathrm{Tr}[\hat{\rho}_{\rm el}^2(t)] = 1 - 2(1 - |\mathcal{F}_{v_g v_e}|^2)|c_{v_g}(t)|^2 |c_{v_e}(t)|^2. \tag{26}$$

The linear entropy of entanglement becomes

$$L_{v_g v_e}(t) = 2(1 - |\mathcal{F}_{v_g v_e}|^2)|c_{v_e}(t)|^2[1 - |c_{v_e}(t)|^2], \tag{27}$$

with $|c_{v_e}(t)|^2$ given by Eq. (23), which means that the characteristic period appearing in the linear entropy evolution is the Rabi period $T^R_{v_e,v_g}$ of the beating between the vibrational levels (v_e,v_g), shown by Eq. (23):

$$T^R_{v_e,v_g} = \frac{\pi}{\Omega_{v_e,v_g}}. \tag{28}$$

By showing that the Rabi period associated to the vibronic coupling is the characteristic time in the evolution of the linear entropy, already this simple model provides insight into the entanglement dynamics during the laser coupling. A beat phenomenon in the reduced-density linear entropy is also signalled in Ref. [15], which analyzes the entanglement of vibrations in triatomic molecules using an algebraic model.

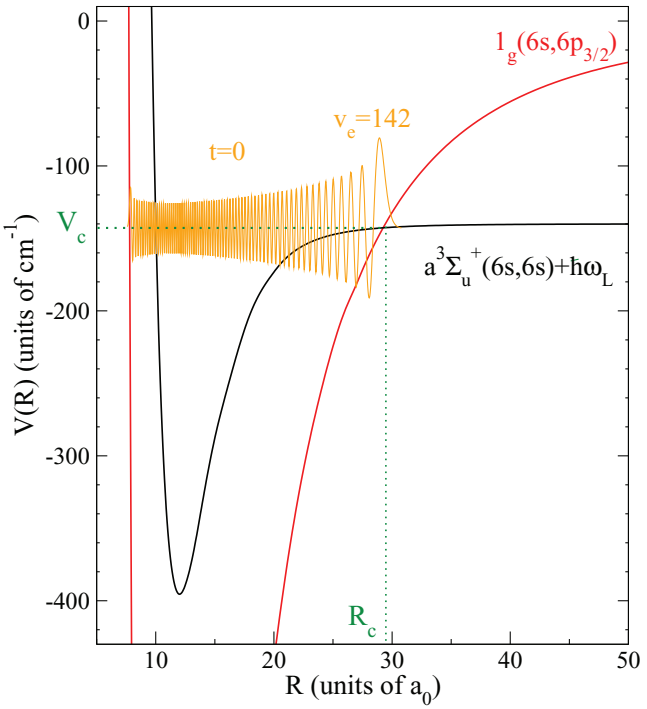

FIG. 1. (Color online) $a^3\Sigma_u{}^+(6s,6s)$ and $1_g(6s,6p_{3/2})$ electronic potentials of Cs_2, dressed with the photon energy $\hbar\omega_L = E_{6p_{3/2}} - E_{6s} - \hbar\Delta_L$ ($\hbar\Delta_L = 140$ cm^{-1}) and crossing at $R_c = 29.3a_0$, $V_c = V_{1_g}(R_c) = V_\Sigma(R_c) = -143$ cm^{-1}. The energy origin is taken to be the dissociation limit $E_{6s+6p_{3/2}} = 0$ of the $1_g(6s+6p_{3/2})$ potential. The initial wave function of the process is the vibrational wave function with $v_e = 142$ of the 1_g electronic state, also represented in the figure.

B. Entanglement dynamics in the case of two electronic states coupled by a laser pulse: Example of $a^3\Sigma_u{}^+(6s,6s) = g$, $1_g(6s,6p_{3/2}) = e$ of the Cs_2 molecule

Here we consider the intramolecular dynamics induced by a laser pulse which couples two electronic states of the Cs_2 molecule. This allows one to follow the temporal dependence of the entanglement measures proposed in the preceding sections and to relate it to the characteristic times of the molecular evolution.

We consider that the electronic channels $e = 1_g(6s,6p_{3/2})$ and $g = a^3\Sigma_u{}^+(6s,6s)$ are coupled by an electric field with amplitude $\mathcal{E}(t) = \mathcal{E}_0 f(t)\cos\omega_L t$, such that the potential curves dressed with the photon energy $\hbar\omega_L$ have a crossing point at R_c (Fig. 1). The time-dependent Schrödinger equation associated with the radial motion of the wave packets $\Psi_e(R,t)$ and $\Psi_g(R,t)$ in the electronic channels, written using the rotating wave approximation with the frequency $\omega_L/2\pi$ [28,29], is

$$i\hbar\frac{\partial}{\partial t}\begin{pmatrix}\Psi_e(R,t)\\ \Psi_g(R,t)\end{pmatrix} = \begin{pmatrix}\hat{\mathbf{T}} + V_e(R) & W_L f(t)\\ W_L f(t) & \hat{\mathbf{T}} + V_g(R)\end{pmatrix}\begin{pmatrix}\Psi_e(R,t)\\ \Psi_g(R,t)\end{pmatrix}. \tag{29}$$

The potentials $V_e(R)$ and $V_g(R)$ are the diabatic electronic potentials crossing at R_c, represented in Fig. 1. $\hat{\mathbf{T}}$ is the kinetic-energy operator and $W_L f(t)$ the coupling between the two

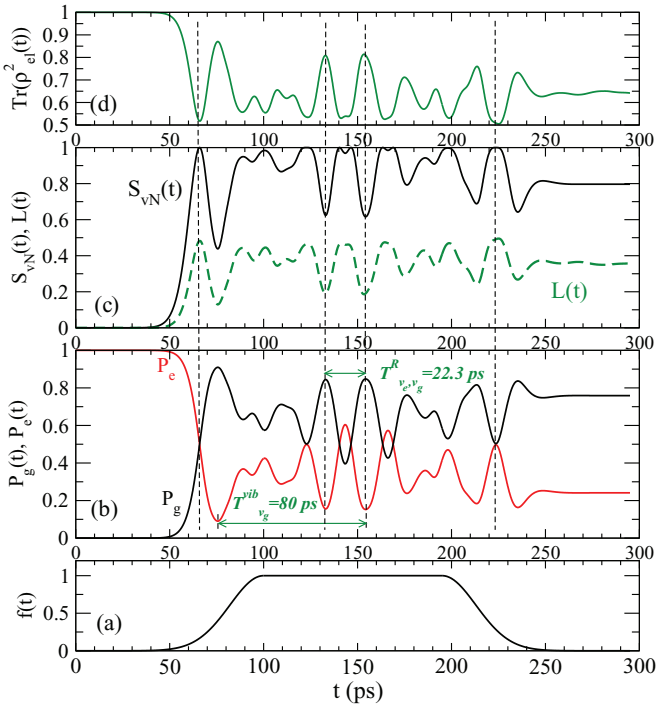

FIG. 2. (Color online) Dynamics of entanglement between electronic and vibrational degrees of freedom for the electronic states $g = a^3\Sigma_u{}^+$ and $e = 1_g$ of Cs_2 (Fig. 1) coupled by a laser pulse. (a) Pulse envelope $f(t)$. (b) Time evolution of the populations $P_g(t)$ and $P_e(t)$. (c) Time evolution of the von Neumann entropy $S_{vN}(t)$ (full line) and linear entropy $L(t)$ (dashed line). (d) Evolution of the purity $\mathrm{Tr}[\hat{\rho}^2_{\mathrm{el}}(t)]$.

channels, with $f(t)$ the temporal envelope of the pulse [shown in Fig. 2(a)]. $W_L = -\frac{1}{2}\mathcal{E}_0 D^{\vec{e}_L}_{ge}$, where $\mathcal{E}_0 = \sqrt{2I/c\epsilon_0}$ is the field amplitude (with I the laser intensity), $\vec{e}_L$ the polarization, and $D^{\vec{e}_L}_{ge}$ the transition dipole moment between the ground and the excited molecular electronic states. If one neglects the R dependence of the transition dipole moment, using a value $D^{\vec{e}_L}_{ge}$ deduced from standard long-range calculations for a linear polarization vector $\vec{e}_L$ [30], for a pulse intensity $I \approx 43$ MW/cm^2 one obtains a coupling $W_L = 13.17$ cm^{-1}. The initial state of the process, represented in Fig. 1, is the vibrational eigenstate $\chi^{v_e=142}_{1_g}(R)$ corresponding to the vibrational level $v_e = 142$ of the excited electronic potential $1_g(6s + 6p_{3/2})$, bound by $E_{v_e} = -140.9$ cm^{-1}.

The dynamics is simulated solving numerically the Schrödinger equation (29), by propagating in time the initial wave function $(\chi^{v_e=142}_{1_g}(R)_0)$ on a spatial grid with length $L_R \approx 370a_0$. The time propagation uses the Chebychev expansion of the evolution operator [31,32] and the mapped sine grid (MSG) method [33,34] to represent the radial dependence of the wave packets. The populations in each electronic state are calculated from the vibrational wave packets $\Psi_e(R,t)$ and $\Psi_g(R,t)$ as $P_{g,e}(t) = \int^{L_R} |\Psi_{g,e}(R',t)|^2 dR'$, with the total population normalized at 1 on the spatial grid $[P_g(t) + P_e(t) = 1]$, and $P_e(0) = 1$.

The evolution of the populations $P_g(t)$, $P_e(t)$ during the pulse is shown in Fig. 2(b). The chosen pulse is sufficiently long (about 200 ps) and strong (the maximum local Rabi period associated with the constant coupling W_L is $T_{\mathrm{Rabi}}(R_c) = \hbar\pi/W_L = 1.27$ ps [29]) to put in evidence typical phenomena such as the beats between various vibrational levels populated by the pulse, and the vibrational motion in the potential wells. Several vibrational levels of each electronic surface having energies close to the energy crossing V_c are populated during the pulse, with typical vibrational periods of 11 ps in the 1_g potential, and between 40 ps and 80 ps in the $a^3\Sigma_u{}^+$ potential. The time scales related to the laser coupling and vibrational motion have been analyzed in detail in Ref. [29]. The time evolution shown in Fig. 2(b) is characterized by inversion of population between the two channels and a Rabi beating with the period $T^R_{v_e,v_g} = 22.3$ ps, specific to the vibrational levels $v_e = 142$ of 1_g and $v_g = 47$ of $a^3\Sigma_u{}^+$, whose vibrational periods are $T^{\mathrm{vib}}_{v_e=142} = 10.8$ ps and $T^{\mathrm{vib}}_{v_g=47} = 80$ ps. In the figure, this last characteristic time appears as related to the revival of Rabi oscillations of maximum amplitude.

The entanglement dynamics is illustrated by the evolution of the von Neumann entropy $S_{vN}(t)$ and the linear entropy $L(t)$, represented in Fig. 2(c). Both show similar time oscillations, with periods which are those of the beats between the populations $P_g(t)$ and $P_e(t)$, dominated here by the Rabi period $T^R_{v_e,v_g} = 22.3$ ps. The equalization of populations between the two electronic channels creates the condition for maximum entanglement $[S_{vN}(t) = 1]$, which is repeatedly realized during the pulse action. Finally, the laser pulse leaves the system in an entangled state $|\Psi_{\mathrm{el,vib}}(t)\rangle$ characterized by a high von Neumann entropy $S_{vN}(t = 300\ \mathrm{ps}) \approx 0.8$.

IV. ENTANGLEMENT BETWEEN ELECTRONIC AND VIBRATIONAL DEGREES OF FREEDOM IN A 3 × N_v SYSTEM

We consider now a bipartite Hilbert space $\mathcal{H} = \mathcal{H}_{\mathrm{el}} \bigotimes \mathcal{H}_{\mathrm{vib}}$ of dimension $3 \times N_v$. We assume the existence of couplings between the three electronic states $|g\rangle$, $|e\rangle$, $|f\rangle$, such that a pure state of $\mathcal{H}$ is created:

$$|\Psi_{\mathrm{el,vib}}(t)\rangle = |g\rangle \bigotimes \sum_{v_g=1}^{N_g} c_{v_g}(t)\left|\chi_{v_g}\right\rangle + |e\rangle \bigotimes \sum_{v_e=1}^{N_e} c_{v_e}(t)\left|\chi_{v_e}\right\rangle + |f\rangle \bigotimes \sum_{v_f=1}^{N_f} c_{v_f}(t)\left|\chi_{v_f}\right\rangle. \quad (30)$$

$\{|\chi_{v_g}\rangle\}_{v_g=\overline{1,N_g}}$, $\{|\chi_{v_e}\rangle\}_{v_e=\overline{1,N_e}}$, and $\{|\chi_{v_f}\rangle\}_{v_f=\overline{1,N_f}}$ are the orthonormal vibrational bases (with dimensions N_g, N_e, N_f, respectively) corresponding to the electronic surfaces g, e, f, and the dimension of the vibrational Hilbert space is $N_v = N_g + N_e + N_f$. The normalization condition $\langle\Psi_{\mathrm{el,vib}}(t)|\Psi_{\mathrm{el,vib}}(t)\rangle = 1$ is expressed by the relation

$$\sum_{v_g}\left|c_{v_g}(t)\right|^2 + \sum_{v_e}\left|c_{v_e}(t)\right|^2 + \sum_{v_f}\left|c_{v_f}(t)\right|^2 = 1, \quad (31)$$

and the density operator $\hat{\rho}_{\mathrm{el,vib}}(t)$ associated with the pure state [as in Eq. (9)] obeys $\hat{\rho}^2_{\mathrm{el,vib}} = \hat{\rho}_{\mathrm{el,vib}}$. Following the line of reasoning employed in Sec. III, the quantification of the entanglement requires the calculation of the electronic reduced density matrix, for which we have to use a complete

orthonormal vibronic basis $\{|j\rangle\}_{j=1,N_v}$, satisfying the orthonormality ($\langle j|j'\rangle = \delta_{jj'}$) and completeness ($\sum_{j=1}^{N_v} |j\rangle\langle j| = \hat{I}_v$) conditions in $\mathcal{H}_{\rm vib}$. This vibronic basis can be associated to a new orthonormal electronic basis $\{|1\rangle,|2\rangle,|3\rangle\}$ in $\mathcal{H}_{\rm el}$, such that the wave function $|\Psi_{\rm el,vib}(t)\rangle$ of the pure bipartite system may be also expressed as

$$|\Psi_{\rm el,vib}(t)\rangle = |1\rangle \bigotimes \sum_{j=1}^{N_v} C_{1j}(t)|j\rangle + |2\rangle \bigotimes \sum_{j=1}^{N_v} C_{2j}(t)|j\rangle + |3\rangle \bigotimes \sum_{j=1}^{N_v} C_{3j}(t)|j\rangle. \quad (32)$$

The complex coefficients C_{1j}, C_{2j}, C_{3j} obey the normalization condition $\sum_{j=1}^{N_v}[|C_{1j}(t)|^2 + |C_{2j}(t)|^2 + |C_{3j}(t)|^2] = 1$.

The reduced density operator $\hat{\rho}_{\rm el}$ is calculated using the vibronic basis $\{|j\rangle\}_{j=1,N_v}$ as shown in Eq. (12), and the reduced density matrix ($\hat{\rho}_{\rm el}$) can be written in the electronic basis $\{|1\rangle,|2\rangle,|3\rangle\}$:

$$(\hat{\rho}_{\rm el}) = \begin{pmatrix} \sum_j |C_{1j}|^2 & \sum_j C_{1j}C_{2j}^* & \sum_j C_{1j}C_{3j}^* \\ \sum_j C_{2j}C_{1j}^* & \sum_j |C_{2j}|^2 & \sum_j C_{2j}C_{3j}^* \\ \sum_j C_{3j}C_{1j}^* & \sum_j C_{3j}C_{2j}^* & \sum_j |C_{3j}|^2 \end{pmatrix}, \quad (33)$$

where the j summations are over $j = \overline{1,N_v}$. It is nevertheless difficult to diagonalize the reduced density matrix (33) and to obtain its eigenvalues in order to get an analytic expression for the von Neumann entropy $S_{vN}(t)$. However, the purity of the reduced density matrix can be calculated using Eq. (33):

$$\begin{aligned} &\mathrm{Tr}\left(\hat{\rho}_{\rm el}^2\right) \\ &= \left(\sum_j |C_{1j}|^2\right)^2 + \left(\sum_j |C_{2j}|^2\right)^2 + \left(\sum_j |C_{3j}|^2\right)^2 \\ &\quad + 2\left(\left|\sum_j C_{1j}C_{2j}^*\right|^2 + \left|\sum_j C_{1j}C_{3j}^*\right|^2 + \left|\sum_j C_{2j}C_{3j}^*\right|^2\right). \end{aligned} \quad (34)$$

Making a choice for the new electronic basis set, as for example

$$\begin{aligned} |1\rangle &= \frac{1}{\sqrt{3}}(|g\rangle + |e\rangle + |f\rangle), \\ |2\rangle &= \frac{1}{\sqrt{6}}(|g\rangle + |e\rangle - 2|f\rangle), \\ |3\rangle &= \frac{1}{\sqrt{2}}(|g\rangle - |e\rangle), \end{aligned} \quad (35)$$

allows one to arrive in Eq. (34) at an expression related to the initial electronic states, based on the electronic populations $P_g(t), P_e(t), P_f(t)$ and overlaps between $|\psi_{g,e,f}(R,t)\rangle$

$$\begin{aligned} &\mathrm{Tr}\left[\hat{\rho}_{\rm el}^2(t)\right] \\ &= P_g^2(t) + P_e^2(t) + P_f^2(t) + 2|\langle\psi_g(R,t)|\psi_e(R,t)\rangle|^2 \\ &\quad + 2|\langle\psi_g(R,t)|\psi_f(R,t)\rangle|^2 + 2|\langle\psi_e(R,t)|\psi_f(R,t)\rangle|^2. \end{aligned} \quad (36)$$

Equation (36) has the same structure as Eq. (22), which now can be regarded as its particular case for only two populated electronic states. The purity given by Eq. (36) is bounded by $\frac{1}{3} \leqslant \mathrm{Tr}(\hat{\rho}_{\rm el}^2) \leqslant 1$, which gives boundaries $0 \leqslant L(t) \leqslant \frac{2}{3}$ for the linear entropy. We shall use Eq. (36) to quantify the electronic-vibrational entanglement in a $3 \times N_v$ molecular system using the reduced linear entropy, $L(t) = 1 - \mathrm{Tr}[\hat{\rho}_{\rm el}^2(t)]$. The next section constitutes an example.

V. ENTANGLEMENT DYNAMICS IN A SYSTEM OF THREE ELECTRONIC STATES COUPLED BY A SEQUENCE OF TWO CHIRPED LASER PULSES

In this section we analyze the production of entanglement [quantified by the linear entropy $L(t)$] in the case of a more complex molecular dynamics, related to a theoretical control scheme proposed to create Cs_2 vibrationally cold molecules [35–37] using the multichannel tunneling observed in the cesium photoassociation spectrum [38].

The scheme, illustrated in Fig. 3, uses a sequence of two chirped laser pulses to couple the electronic potentials $a^3\Sigma_u^+(6s,6s) = g$ and $0_g^-(6s,6p_{3/2}) = e$ of a Cs_2 cold molecule at large interatomic distances ($R_1 \approx 94a_0$), as well as at small distances ($R_2 \approx 15.6a_0$), in order to capture vibrational population in low vibrational levels of the electronic potentials. Moreover, the $0_g^-(6s,6p_{3/2}) = e$ state (having a

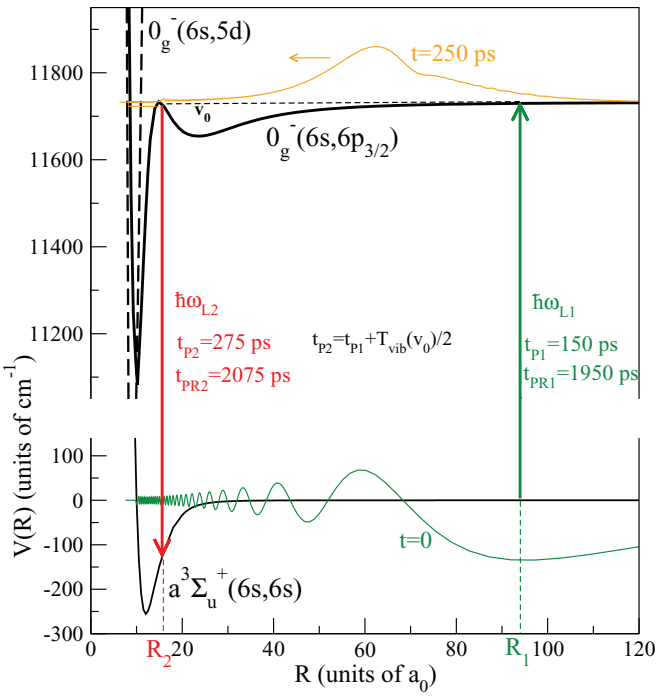

FIG. 3. (Color online) Electronic potentials $a^3\Sigma_u^+(6s,6s) = g$, $0_g^-(6s,6p_{3/2}) = e$, and $0_g^-(6s,5d) = f$ of the Cs_2 molecule, coupled by a sequence of two chirped laser pulses (see also Fig. 4) with central frequencies $\omega_{L1}/2\pi$ and $\omega_{L2}/2\pi$, and by a nonadiabatic coupling (to be seen in the crossing of e and f electronic surfaces at small interatomic distances of about $10a_0$). The initial state at $t = 0$ (a loosely bound vibrational state in $g = a^3\Sigma_u^+$) is also shown, as well as the vibrational wave packet created by the first pulse in the e state, at $t = 250$ ps.

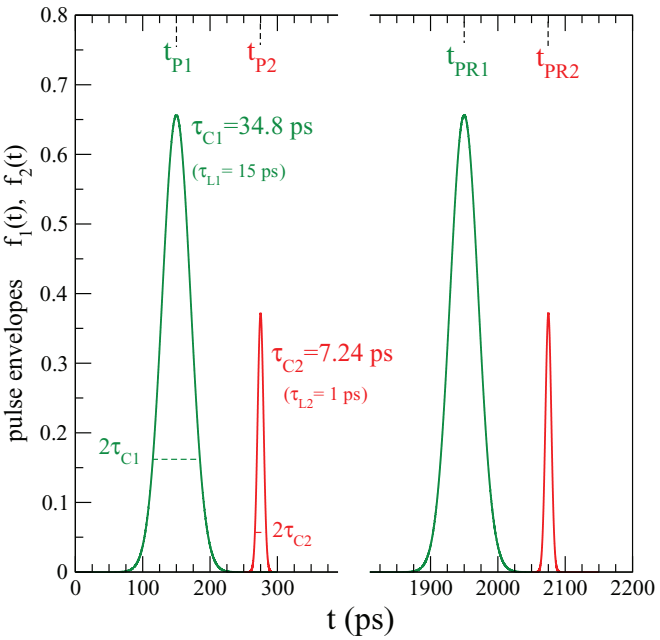

FIG. 4. (Color online) The Gaussian temporal envelopes $f_1(t)$, $f_2(t)$ of the chirped laser pulses which couple the electronic potentials in Fig. 3. The maximum of an envelope is at $f(t_P) = \sqrt{\tau_L/\tau_C}$. The first sequence is made of two pulses centered in $t_{P1} = 150$ ps and $t_{P2} = 275$ ps. The repetition of the sequence after 1800 ps is also shown ($t_{PR1} = 1950$ ps and $t_{PR2} = 2075$ ps).

double-well potential) is coupled in the inner well region to the $0_g^-(6s,5d) = f$ electronic state, through a nonadiabatic coupling generated by the spin-orbit interaction [36]. The first chirped pulse, with central frequency $\omega_{L1}/2\pi$ ($\hbar\omega_{L1} = 11\,729.66$ cm^{-1}) at $t_{P1} = 150$ ps couples $a^3\Sigma_u^+(6s,6s)$ and $0_g^-(6s,6p_{3/2})$ at large interatomic distances ($R_1 \approx 94a_0$). We consider as initial state of the process the "last bound state" of the $a^3\Sigma_u^+(6s,6s)$ potential obtained on a spatial grid of about $1060a_0$. Its wave function (partially visible in Fig. 3) extends up to about $350a_0$ and has a maximum at R_1, being an advantageous choice for the simulation of a cold photoassociation process. Operating on this initial state, the first pulse creates a vibrational wave packet around the vibrational level $v_0 = 98$ of the $0_g^-(6s,6p_{3/2})$ outer well [35], which begins to move to small distances in the $0_g^-(6s+6p_{3/2})$ double well (see Fig. 3). The second delayed pulse, with $\hbar\omega_{L2} = 11\,856.66$ cm^{-1} and $t_{P2} = 275$ ps [37], induces a coupling in the zone of the $0_g^-(6s,6p_{3/2})$ double well barrier ($R_2 \approx 15.6a_0$), controlling the tunneling in the $0_g^-(6s,6p_{3/2})$ potential coupled radially at small interatomic distances ($\approx 10a_0$) with the $0_g^-(6s,5d)$ potential, and transferring population in low vibrational levels of the $a^3\Sigma_u^+(6s,6s)$ state. The theoretical model and the choice of the chirped pulses are described in detail in Refs. [35,37]. Our present calculations include in the model the nonadiabatic coupling at short distances between the $0_g^-(6s,6p_{3/2})$ and $0_g^-(6s,5d)$ potentials, and the repetition of the pulses sequence after 1800 ps (see Fig. 4). These factors were not previously taken into account and, as we will show, they do contribute in the entanglement dynamics.

The succession of pulses considered in this work is represented in Fig. 4. Each pulse has a Gaussian envelope $f(t)$ and negative linear chirp, being described by an electric field $E(t) = E_0 f(t)\cos[\omega_L t + \varphi(t)]$, where $\omega_L/2\pi$ is the central frequency reached at $t = t_P$, and $\varphi(t)$ a phase which is a quadratic function of time. The Gaussian envelope $f(t) = \sqrt{\tau_L/\tau_C}\exp\{-2\ln 2[(t-t_P)/\tau_C]^2\}$ is centered at $t = t_P$, having the temporal width τ_C defined as the full width at half maximum (FWHM) of the temporal intensity profile $E_0^2 f^2(t)$. The maximum of $f(t)$ is at $f(t_P) = \sqrt{\tau_L/\tau_C}$, where τ_L is the temporal width of the transform limited pulse (before chirping). Such a pulse is characterized by several parameters belonging to the spectral and temporal domains, which are carefully chosen in order to control the system evolution (a detailed analysis is contained in Refs. [33,37]).

The vibrational dynamics is obtained by solving numerically the time-dependent Schrödinger equation associated with the radial motion of the vibrational wave packets. For each pulse, the coupling between electronic surfaces is treated by using the rotating wave approximation with the corresponding carrier frequency $\omega_L/2\pi$. Then, for a given pulse, the coupled equations for the evolution of the radial wave functions $\Psi^{\omega}_{g,e,f}(R,t)$ in the dressed diabatic potentials $V'_e(R) = V_e(R)$, $V'_f(R) = V_f(R)$, and $V'_g(R) = V_g(R) + \hbar\omega_L$, can be written as

$$i\hbar\frac{\partial}{\partial t}\begin{pmatrix}\Psi^{\omega}_e(R,t)\\ \Psi^{\omega}_f(R,t)\\ \Psi^{\omega}_g(R,t)\end{pmatrix} = \begin{pmatrix}\hat{\mathbf{T}}+V'_e(R) & V_{12}(R) & -W_L f(t)e^{-i\varphi(t)}\\ V_{12}(R) & \hat{\mathbf{T}}+V'_f(R) & 0\\ -W_L f(t)e^{i\varphi(t)} & 0 & \hat{\mathbf{T}}+V'_g(R)\end{pmatrix}\begin{pmatrix}\Psi^{\omega}_e(R,t)\\ \Psi^{\omega}_f(R,t)\\ \Psi^{\omega}_g(R,t)\end{pmatrix}. \quad (37)$$

Similar to the example analyzed in Sec. III B, $\hat{\mathbf{T}}$ is the kinetic-energy operator and $W_L = -\mathcal{E}_0 D_{ge}/2$ is the laser coupling determined by the laser intensity I ($\mathcal{E}_0 = \sqrt{2I/c\epsilon_0}$) and the transition dipole moment $D_{ge}/2$. The Cs_2 molecular potential curves used in the present work were described in Refs. [36,38]. The nonadiabatic coupling between $0_g^-(6s,6p_{3/2})$ and $0_g^-(6s,5d)$ electronic potentials is modeled using a radial coupling $V_{12}(R)$ of Gaussian form [36] in the Hamiltonian matrix of Eq. (37). The numerical methods used to solve Eq. (37) are those already mentioned in Sec. III B.

The populations $P_g(t)$, $P_e(t)$, $P_f(t)$ in each electronic state are calculated from the vibrational wave packets as

$$P_{g,e,f}(t) = \int^{L_R} \left|\Psi^{\omega}_{g,e,f}(R',t)\right|^2 dR', \quad (38)$$

where $L_R = 1060a_0$ is the length of the spatial grid used to solve Eq. (37) by wave-packet propagation. The total

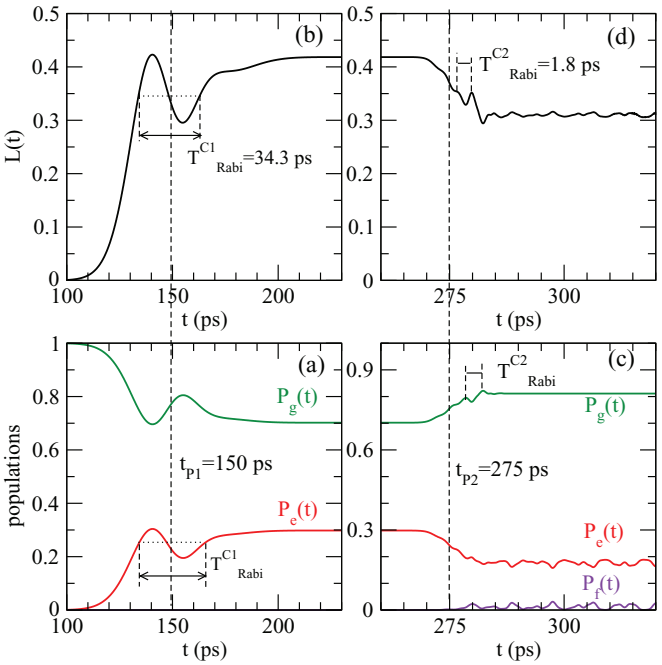

FIG. 5. (Color online) Time evolution of the linear entropy and electronic populations during the first sequence of pulses (see Fig. 4). (a),(b) The population evolution in the three electronic channels, and the linear entropy evolution, respectively, during the first chirped pulse. (c),(d) The population evolution and linear entropy evolution, respectively, during the second chirped pulse.

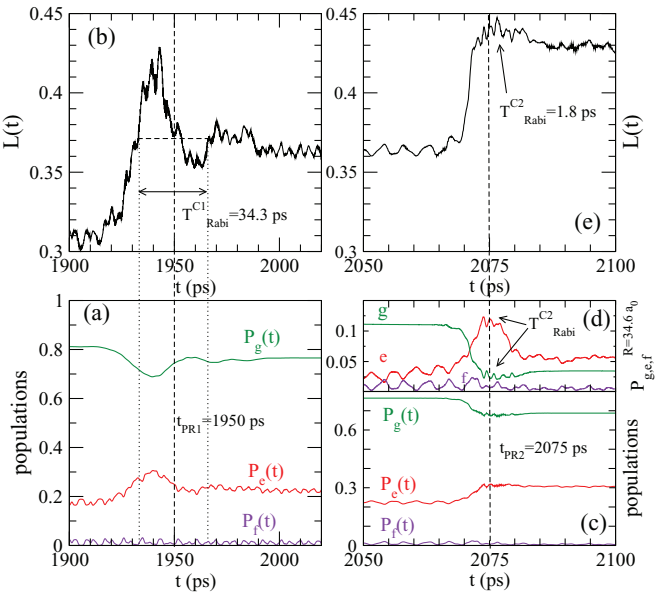

FIG. 6. (Color online) Time evolution of the linear entropy and electronic populations during the repetition of the pulse sequence after 1800 ps (see Fig. 4). (a),(b) The population evolution in the three electronic channels, and the linear entropy evolution, respectively, during the repetition of the first chirped pulse. (c) Population evolution during the repetition of the second chirped pulse. (d) Evolution of the partial populations $P^{R=34.6a_0}_{g,e,f} = \int^{R=34.6a_0} |\Psi_{g,e,f}(R',t)|^2 dR'$ during the repetition of the second chirped pulse. (e) Evolution of the linear entropy during the repetition of the second chirped pulse.

population is normalized at 1 on the spatial grid $[P_g(t) + P_e(t) + P_f(t) = 1]$, with $P_g(t = 0) = 1$.

The linear entropy, $L(t) = 1 - \mathrm{Tr}[\hat{\rho}^2_{el}(t)]$, calculated with Eq. (36), is used to characterize the entanglement dynamics during the whole process. Figures 5 and 6 show the evolution of the linear entropy and electronic populations during each pulse. In Fig. 7 is represented the overall linear entropy evolution. In the following, we will analyze these results.

In the population evolution appears the chirped Rabi period [35], which is a characteristic time associated with the action of a chirped pulse:

$$T^C_{\mathrm{Rabi}}(t_P) = \sqrt{\frac{\tau_C}{\tau_L}}\frac{\hbar\pi}{W_L}. \tag{39}$$

The first chirped pulse, characterized by a coupling strength $W_{L1} = 0.74$ cm^{-1} and a chirped Rabi period $T^{C1}_{\mathrm{Rabi}}(t_{P1}) = 34.3$ ps, acts at large R distances and produces a transfer of population from the g electronic state to the e state: the characteristic period $T^{C1}_{\mathrm{Rabi}}(t_{P1})$ appears clearly in the evolution of the populations and linear entropy, in Figs. 5(a) and 5(b). The second pulse comes with a coupling strength $W_{L2} = 24.69$ cm^{-1} and a chirped Rabi period $T^{C2}_{\mathrm{Rabi}}(t_{P2}) = 1.8$ ps, and operates an exchange of populations at much smaller $R \leqslant 35a_0$ distances, bringing population back to the ground electronic state g, but in strongly bound vibrational levels. Its characteristic Rabi period $T^{C2}_{\mathrm{Rabi}}(t_{P2})$ can be distinguished in the evolution of the populations and linear entropy, in Figs. 5(c) and 5(d), but with a smaller amplitude, due to the smaller amount of transferred population. On the other hand, during the second pulse which brings population into the inner zone, the evolution of the populations and linear entropy begins to show the beats due to the nonadiabatic coupling between the e and f states.

The evolution during the repetition of the pulse sequence after 1800 ps is represented in Figs. 6(a) and 6(b) for the first pulse and in Figs. 6(c)–6(e) for the second pulse. As the second pulse operates at small distances R, it appears that to understand its effects one has to represent also the partial populations $P^{R=34.6a_0}_{g,e,f} = \int^{R=34.6a_0} |\Psi_{g,e,f}(R',t)|^2 dR'$, calculated by integrating the vibrational wave packets up to $R = 34.6a_0$ [Fig. 6(d)]. Then, the chirped Rabi period $T^{C2}_{\mathrm{Rabi}}(t_{P2})$ may be easily identified in their evolution, as in the linear entropy evolution presented in Fig. 6(e).

The repetition of the first pulse feels the "void" left in the g initial wave function by the initial first pulse [see Fig. 8(a)], and as a result less population is transferred from the ground state g to the excited state e at large distances [Fig. 6(a)]. Nevertheless, by bringing closer the electronic populations P_g and P_e, the first pulse (the initial and its repetition) leads to an increase of the linear entropy (Fig. 7). On the other hand, the second pulse in the sequence (which operates at small distances) has different effects initially and in its repetition. In the first stage, it transfers population in low vibrational levels of the ground state g, which has a "purification effect" on the overall state, lowering the linear entropy [see Figs. 5(c) and 5(d) and 7]. In contrast, its repetition transfers population back in the inner well of the excited state e [Figs. 6(c) and 6(d)], bringing even closer the electronic populations and increasing $L(t)$ [Fig. 6(e)]. Therefore, it appears that the repetition of

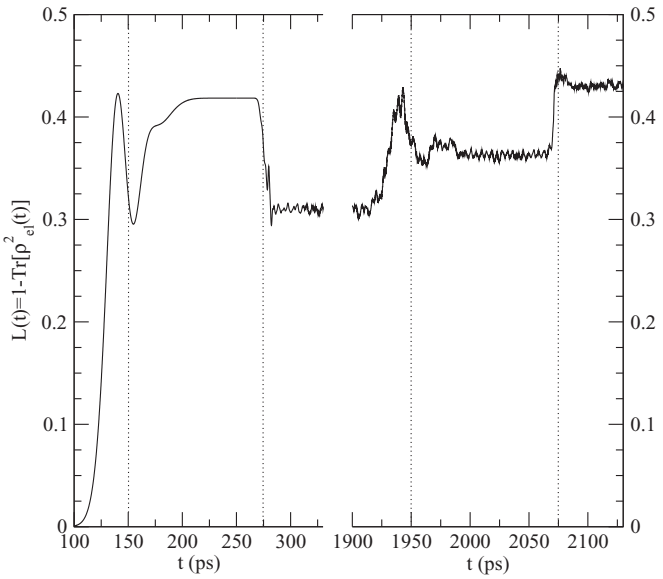

FIG. 7. Dynamics of entanglement: time evolution of the linear entropy $L(t) = 1 - \mathrm{Tr}[\hat{\rho}_{\mathrm{el}}^2(t)]$ during the pulse sequence represented in Fig. 4. The vertical dotted lines indicate the instants t_{P1}, t_{P2}, t_{PR1}, t_{PR2} corresponding to the maximum of every pulse envelope, as it is shown in Fig. 4.

the pulse sequence is significant to the overall picture, which is best seen in the evolution of the linear entropy during the process (Fig. 7).

The succession of pulses creates a final state $|\Psi_{\mathrm{el,vib}}(t)\rangle$ with significant entanglement, if we take into account that the linear entropy is maximally bounded by 2/3, and here $L(t)$ attains 0.42. The vibrational components $\psi_{g,e,f}(R,t)$ of the pure entangled state $|\Psi_{\mathrm{el,vib}}(t)\rangle$, according to Eq. (30), are shown in Fig. 8 [other decompositions of $|\Psi_{\mathrm{el,vib}}(t)\rangle$ are equally possible, as in Eq. (32)].

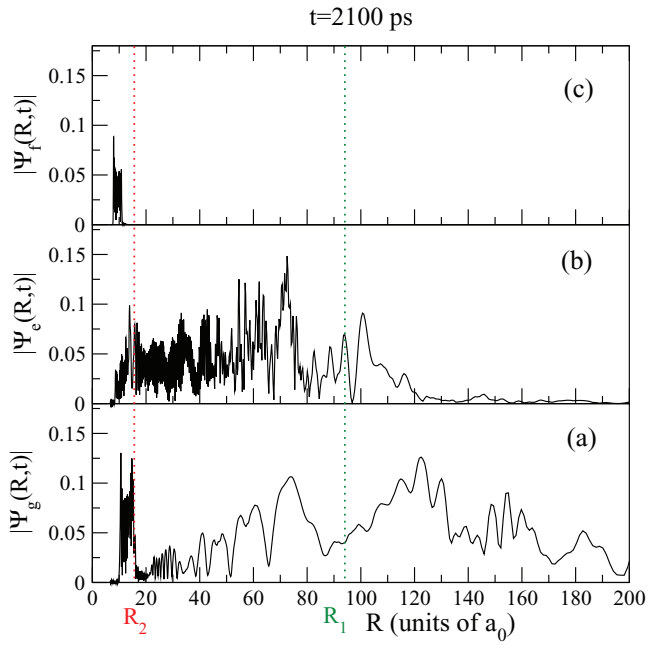

FIG. 8. (Color online) Vibrational components $\psi_{g,e,f}(R,t)$ of the pure entangled state $|\Psi_{\mathrm{el,vib}}(t)\rangle = |g\rangle \bigotimes |\psi_g(t)\rangle + |e\rangle \bigotimes |\psi_e(t)\rangle + |f\rangle \bigotimes |\psi_f(t)\rangle$ created by the succession of pulses at $t = 2100$ ps.

VI. CONCLUSION

We have investigated the entanglement between electronic and nuclear degrees of freedom produced by vibronic couplings in pure states of the Hilbert space $\mathcal{H} = \mathcal{H}_{\mathrm{el}} \bigotimes \mathcal{H}_{\mathrm{vib}}$. Expressions for the von Neumann entanglement entropy and the reduced linear entropy were derived for the $2 \times N_v$ and $3 \times N_v$ cases of the bipartite entanglement (el $\bigotimes$ vib), relating these entanglement measures to quantities specific to the intramolecular dynamics, such as the electronic populations and the vibronic coherences.

The entanglement dynamics was analyzed in two cases of laser coupling between electronic states, using as an example the Cs_2 molecule. In the first case, treated in Sec. III B, we have simulated the vibrational dynamics for two electronic states of the Cs_2 molecule, $a^3\Sigma_u^+(6s,6s)$ and $1_g(6s,6p_{3/2})$, which are coupled by a laser pulse. We show that the Rabi period due to the vibronic laser coupling is also a characteristic time in the evolution of the von Neumann entropy and of the reduced linear entropy. The pulse creates the conditions for the equalization of population between the two electronic channels, producing an electronically maximally entangled state in several stages of the temporal evolution.

The second case, described in Sec. V, is related to a theoretical control scheme proposed to create Cs_2 vibrationally cold molecules using a multichannel tunneling in the $0_g^-(6s,6p_{3/2})$ and $0_g^-(6s,5d)$ electronic states coupled through a nonadiabatic coupling generated by the spin-orbit interaction. The scheme employs three electronic states [$a^3\Sigma_u^+(6s,6s)$, $0_g^-(6s,6p_{3/2})$, and $0_g^-(6s,5d)$] coupled by a sequence of two chirped laser pulses. In addition to previous treatments, we have introduced in the simulation of the dynamics the nonadiabatic coupling between $0_g^-(6s,6p_{3/2})$ and $0_g^-(6s,5d)$ at short distances, and the repetition of the pulse sequence. In these conditions we have analyzed the entanglement dynamics quantified by the reduced linear entropy. The chirped Rabi period characteristic to each pulse can be identified in the linear entropy evolution, as well as the beats period due to the nonadiabatic radial coupling between the tunneling channels $0_g^-(6s,6p_{3/2})$ and $0_g^-(6s,5d)$. We have shown that the repetition of the pulse sequence has considerable influence on the process, diminishing the purification effect of the first sequence and increasing the entanglement in the final state.

In both cases, the results show that the characteristic times related to the vibronic couplings and the vibrational motion are present in the entanglement structure. The linear entropy, calculated from the purity of the electronic reduced density matrix, appears as an interesting sensor for the correlations between the electronic channels, emphasizing explicitly the role played by the vibronic coherences. This property could qualify the linear entropy as a useful reference in control schemes of the molecular coherence and entanglement [39].

In a molecule controlled by laser pulses which leave more than one electronic state populated, electronic-vibrational entanglement is always produced. The amount of entanglement will depend on the "entangling power" of the quantum evolution [40], which is directed here by the laser pulses, and could, in principle, be controlled.

Molecules are systems whose entanglement properties are beginning to be explored. Many phenomena are expected to contribute to the intramolecular dynamics and they could be interrogated in future developments regarding electronic-nuclear entanglement in isolated molecules: electronic energy relaxation, vibrational energy redistribution and relaxation, and various coupling mechanisms [41]. We hope that the present work will help in these possible developments, and also in future studies aiming to investigate the environment effects and the control of entanglement in molecules.

ACKNOWLEDGMENTS

I am grateful to O. Patu for the critical reading of the manuscript. This work was supported by the LAPLAS 3 39N Research Program of the Romanian Ministry of Education and Research.

[1] R. Horodecki, P. Horodecki, M. Horodecki, and K. Horodecki, Rev. Mod. Phys. **81**, 865 (2009).
[2] M. A. Nielsen and I. L. Chuang, *Quantum Computation and Quantum Information* (Cambridge University Press, Cambridge, 2000).
[3] D. J. Wineland, Rev. Mod. Phys. **85**, 1103 (2013).
[4] S. Haroche, Rev. Mod. Phys. **85**, 1083 (2013).
[5] D. Jaksch, H. J. Briegel, J. I. Cirac, C. W. Gardiner, and P. Zoller, Phys. Rev. Lett. **82**, 1975 (1999); I. Bloch, Nature (London) **453**, 1016 (2008); A. J. Daley, H. Pichler, J. Schachenmayer, and P. Zoller, Phys. Rev. Lett. **109**, 020505 (2012).
[6] A. Widera, O. Mandel, M. Greiner, S. Kreim, T. W. Hänsch, and I. Bloch, Phys. Rev. Lett. **92**, 160406 (2004).
[7] P. O. Schmidt, T. Rosenband, C. Langer, W. M. Itano, J. C. Bergquist, and D. J. Wineland, Science **309**, 749 (2005).
[8] C. F. Roos, M. Chwalla, K. Kim, M. Riebe, and R. Blatt, Nature (London) **443**, 316 (2006).
[9] D. DeMille, Phys. Rev. Lett. **88**, 067901 (2002); S. F. Yelin, D. DeMille, and R. Côté, in *Cold Molecules: Theory, Experiment and Applications*, edited by R. V. Krems, W. C. Stwalley, and B. Friedrich (Taylor and Francis, Boca Raton, 2009), pp. 629–648; F. Herrera, S. Kais, and K. B. Whaley, arXiv:atom-ph/1302.6444.
[10] M. Tichy, F. Mintert, and A. Buchleitner, J. Phys. B **44**, 192001 (2011).
[11] O. Osenda and P. Serra, Phys. Rev. A **75**, 042331 (2007); J. P. Coe and I. D'Amico, J. Phys. Conf. Ser. **254**, 012010 (2010); D. Manzano, A. R. Plastino, J. S. Dehesa, and T. Koga, J. Phys. A: Math. Theor. **43**, 275301 (2010); R. J. Yañez, A. R. Plastino, and J. S. Dehesa, Eur. Phys. J. D **56**, 141 (2010); J. S. Dehesa, T. Koga, R. J. Yañez, A. R. Plastino, and R. O. Esquivel, J. Phys. B **45**, 015504 (2012); G. Benenti, S. Siccardi, and G. Strini, Eur. Phys. J. D **67**, 83 (2013); Y. C. Lin, C. Y. Lin, and Y. K. Ho, Phys. Rev. A **87**, 022316 (2013).
[12] M. Roghani, H.-P. Breuer, and H. Helm, Phys. Rev. A **85**, 012313 (2012).
[13] T. Opatrný and G. Kurizki, Phys. Rev. Lett. **86**, 3180 (2001); C. Gneiting and K. Hornberger, Phys. Rev. A **81**, 013423 (2010); R. O. Esquivel, N. Flores-Gallegos, M. Molina-Espíritu, A. R. Plastino, J. C. Angulo, J. Antolín, and J. S. Dehesa, J. Phys. B **44**, 175101 (2011); X. Li and M. Shapiro, Phys. Rev. A **85**, 043413 (2012).
[14] M. Lombardi and A. Matzkin, Phys. Rev. A **73**, 062335 (2006).
[15] X. W. Hou, J. H. Chen, and Z. Q. Ma, Phys. Rev. A **74**, 062513 (2006); L. Zhai and Y. Zheng, *ibid.* **88**, 012504 (2013).
[16] R. Zadoyan, D. Kohen, D. A. Lidar, and V. A. Apkarian, Chem. Phys. **266**, 323 (2001); C. M. Tesch and R. de Vivie-Riedle, Phys. Rev. Lett. **89**, 157901 (2002); J. P. Palao and R. Kosloff, *ibid.* **89**, 188301 (2002); J. Vala, Z. Amitay, B. Zhang, S. R. Leone, and R. Kosloff, Phys. Rev. A **66**, 062316 (2002); C. Gollub, U. Troppmann, and R. de Vivie-Riedle, New J. Phys. **8**, 48 (2006); U. Troppmann, C. Gollub, and R. de Vivie-Riedle, *ibid.* **8**, 100 (2006); T. Cheng and A. Brown, J. Chem. Phys. **124**, 034111 (2006); M. Zhao and D. Babikov, *ibid.* **126**, 204102 (2007); K. Mishima, K. Tokumo, and K. Yamashita, Chem. Phys. **343**, 61 (2008).
[17] E. Sjöqvist, Int. J. Quantum Chem. **77**, 526 (2000).
[18] L. K. McKemmish, R. H. McKenzie, N. S. Hush, and J. R. Reimers, J. Chem. Phys. **135**, 244110 (2011).
[19] H. Fujisaki, Phys. Rev. A **70**, 012313 (2004).
[20] H. Lefebvre-Brion and R. W. Field, *The Spectra and Dynamics of Diatomic Molecules* (Elsevier Academic, Amsterdam, 2004).
[21] F. Mintert, A. Carvalho, M. Kus, and A. Buchleitner, Phys. Rep. **415**, 207 (2005).
[22] V. Vedral, Rev. Mod. Phys. **74**, 197 (2002).
[23] V. Vedral and M. B. Plenio, Phys. Rev. A **57**, 1619 (1998).
[24] C. H. Bennett, H. J. Bernstein, S. Popescu, and B. Schumacher, Phys. Rev. A **53**, 2046 (1996).
[25] G. Vidal, J. Mod. Opt. **47**, 355 (2000).
[26] S. M. Barnett, *Quantum Information* (Oxford University Press, Oxford, 2009).
[27] G. Jaeger, *Quantum Information. An Overview* (Springer, New York, 2007).
[28] M. Vatasescu, O. Dulieu, R. Kosloff, and F. Masnou-Seeuws, Phys. Rev. A **63**, 033407 (2001).
[29] M. Vatasescu, J. Phys. B **42**, 165303 (2009).
[30] M. Vatasescu, Ph.D. thesis, Université Paris XI, 1999.
[31] R. Kosloff, Annu. Rev. Phys. Chem. **45**, 145 (1994).
[32] R. Kosloff, in *Dynamics of Molecules and Chemical Reactions*, edited by R. E. Wyatt and J. Z. Zhang (Marcel Dekker, New York, 1996), pp. 185–230.
[33] E. Luc-Koenig, M. Vatasescu, and F. Masnou-Seeuws, Eur. Phys. J. D **31**, 239 (2004).
[34] K. Willner, O. Dulieu, and F. Masnou-Seeuws, J. Chem. Phys. **120**, 548 (2004).
[35] E. Luc-Koenig, R. Kosloff, F. Masnou-Seeuws, and M. Vatasescu, Phys. Rev. A **70**, 033414 (2004).

[36] M. Vatasescu, C. M. Dion, and O. Dulieu, J. Phys. B **39**, S945 (2006).
[37] M. Vatasescu, Nucl. Instrum. Methods Phys. Res., Sect. B **279**, 8 (2012).
[38] M. Vatasescu, O. Dulieu, C. Amiot, D. Comparat, C. Drag, V. Kokoouline, F. Masnou-Seeuws, and P. Pillet, Phys. Rev. A **61**, 044701 (2000).
[39] F. Lucas, F. Mintert, and A. Buchleitner, Phys. Rev. A **88**, 032306 (2013).
[40] P. Zanardi, C. Zalka, and L. Faoro, Phys. Rev. A **62**, 030301 (2000).
[41] A. Tramer, C. Jungen, and F. Lahmani, *Energy Dissipation in Molecular Systems* (Springer, Berlin, 2005).